The Casimir effect in Abelian and Non-Abelian lattice gauge theories: induced phase transitions and new boundary states

Maxim Chernodub[1], Vladimir Goy[2], Alexander Molochkov[2], **Aleksei Tanashkin**[2]

Based on arXiv:2203.14922, arXiV:2302.00376

February 28, 2023

[1] *Institut Denis Poisson, Université de Tours, Tours, France*
[2] *Pacific Quantum Center, Far Eastern Federal University, Vladivostok, Russia*

Infinite and Finite Nuclear Matter (INFINUM-2023)
BLTP, JINR, Dubna

The Casimir effect

The emergence of attractive force F_C between two conducting metallic plates in vacuum.

Predicted in 1948 by Casimir.

Indirect experimental evidence in 1958.

The direct experiment in 1997 (Lamoreaux).

$$\frac{F_C}{A} = -\frac{\pi^2}{240} \cdot \frac{\hbar c}{a^4}$$

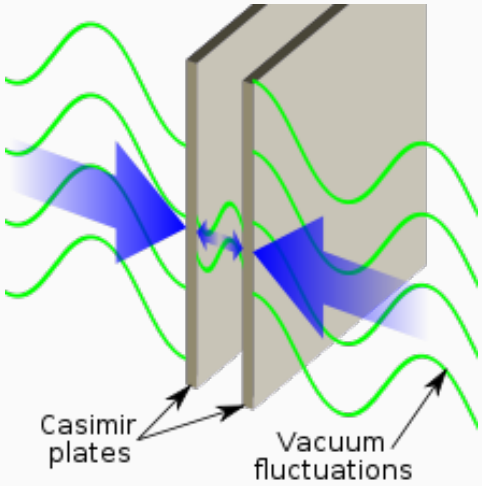

Figure 1: The schematic picture of Casimir effect. Wikipedia

Motivation

- Systems with boundaries
  - MIT bag model
  - Four-fermion theory with the presence of reflective boundaries
  - $\mathbb{C}P^{N-1}$ model with Dirichlet boundary conditions
  - Quenched QCD with Dirichlet boundary conditions
- The effect of boundaries on vacuum structure of the theory

Casimir boundary conditions on the lattice

Action

$$S_{\mathrm{G}} = \beta \sum_{n \in \Lambda} \sum_{\mu < \nu} (1 - \tfrac{1}{N} \mathrm{Re}\,\mathrm{tr}\, U_P)$$

$$U_{P_{x,\mu\nu}} = U_{x,\mu} U_{x+\hat{\mu},\nu} U^{\dagger}_{x+\hat{\nu},\mu} U^{\dagger}_{x,\nu}$$

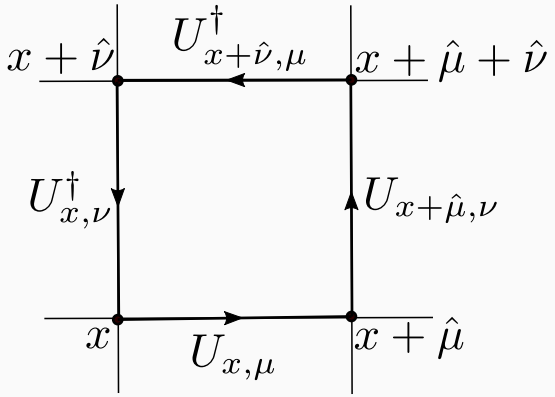

Figure 2: The plaquette variable at site x.

Casimir boundary conditions on the lattice

Action

$$S_G = \beta \sum_{n \in \Lambda} \sum_{\mu < \nu} (1 - \tfrac{1}{N} \mathrm{Re}\,\mathrm{tr}\, U_P)$$

$$U_{P_{x,\mu\nu}} = U_{x,\mu} U_{x+\hat{\mu},\nu} U^{\dagger}_{x+\hat{\nu},\mu} U^{\dagger}_{x,\nu}$$

Casimir boundary conditions

$$E^{(a)}_{\parallel}(x)\Big|_{x \in S} = B^{(a)}_{\perp}(x)\Big|_{x \in S} = 0,$$

$$a = 1, \ldots, N_c^2 - 1$$

$$\beta \to \beta_P = \beta[1 + (\varepsilon - 1)\delta_{P,\mathcal{V}}]$$

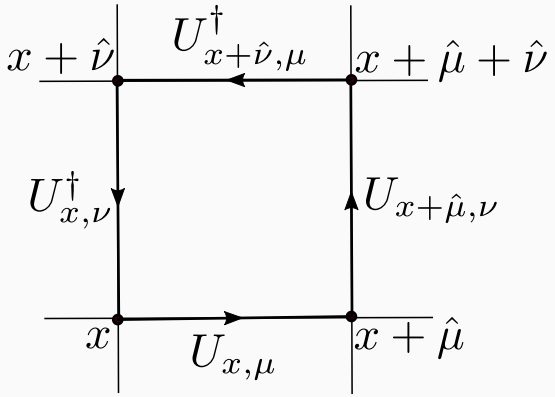

Figure 2: The plaquette variable at site x.

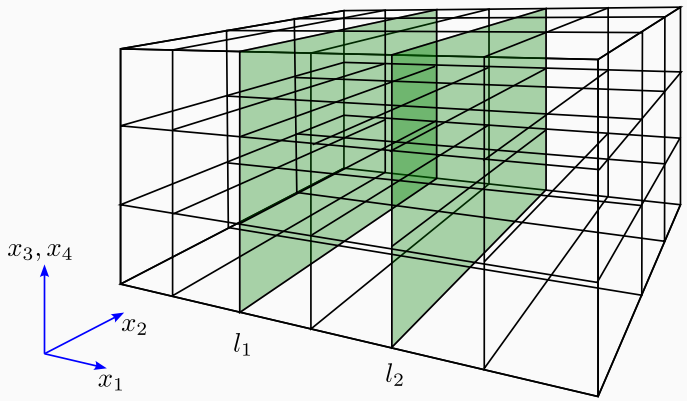

Figure 3: The position of Casimir plates.

Monopoles in cQED on the lattice

Compact QED Action

$$S_{\mathrm{cQED}}[\theta] = \beta \sum_{n \in \Lambda} \sum_{\mu < \nu} (1 - \cos \theta_P)$$

$$\theta_{P_{x,\mu\nu}} = \theta_{x,\mu} + \theta_{x+\hat{\mu},\nu} - \theta_{x+\hat{\nu},\mu} - \theta_{x,\nu}$$

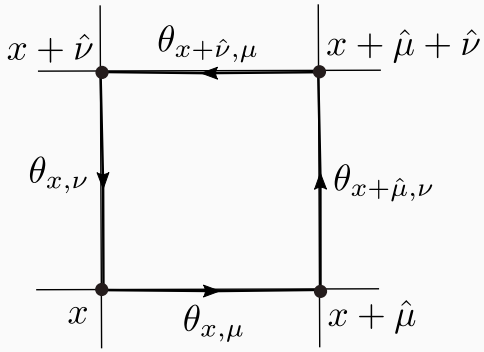

Figure 4: The plaquette angle at site x.

Monopoles in cQED on the lattice

Compact QED Action

$$S_{\mathrm{cQED}}[\theta] = \beta \sum_{n\in\Lambda} \sum_{\mu<\nu} (1 - \cos\theta_P)$$

$$\theta_{P_{x,\mu\nu}} = \theta_{x,\mu} + \theta_{x+\hat{\mu},\nu} - \theta_{x+\hat{\nu},\mu} - \theta_{x,\nu}$$

Monopoles

$$\bar{\theta}_P = \theta_P + 2\pi k_P \in [-\pi, \pi), \qquad k_P \in \mathbb{Z}$$

$$j_{x,\mu} = \frac{1}{2\pi} \sum_{P\in\partial C_{x,\mu}} \bar{\theta}_P \in \mathbb{Z}$$

$$\rho = \frac{1}{\mathrm{Vol}_4} \sum_{x,\mu} |j_{x,\mu}|$$

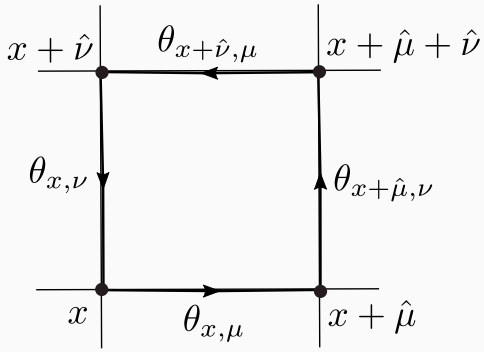

Figure 4: The plaquette angle at site x.

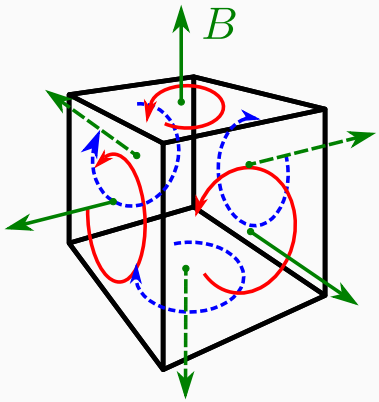

Figure 5: Schematic illustration of monopole charge on the lattice.

Monopoles in cQED on the lattice

Compact QED Action

$$S_{\mathrm{cQED}}[\theta] = \beta \sum_{n\in\Lambda} \sum_{\mu<\nu} (1 - \cos\theta_P)$$

$$\theta_{P_{x,\mu\nu}} = \theta_{x,\mu} + \theta_{x+\hat{\mu},\nu} - \theta_{x+\hat{\nu},\mu} - \theta_{x,\nu}$$

Monopoles

$$\bar{\theta}_P = \theta_P + 2\pi k_P \in [-\pi, \pi), \qquad k_P \in \mathbb{Z}$$

$$j_{x,\mu} = \frac{1}{2\pi} \sum_{P\in\partial C_{x,\mu}} \bar{\theta}_P \in \mathbb{Z}$$

$$\rho = \frac{1}{\mathrm{Vol}_4} \sum_{x,\mu} |j_{x,\mu}|$$

The presence of monopole condensate leads to linear confinement of electric charges.

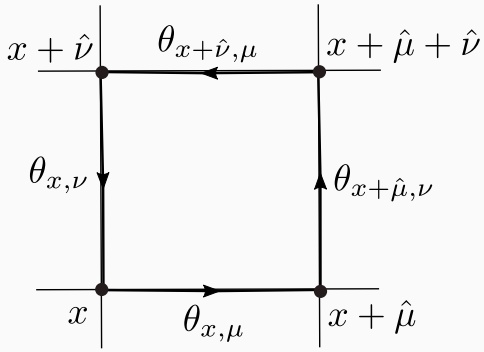

Figure 4: The plaquette angle at site x.

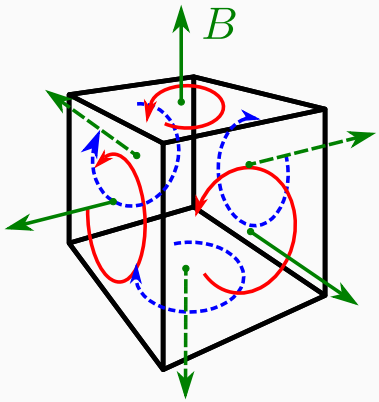

Figure 5: Schematic illustration of monopole charge on the lattice.

The phase transition in the absence of plates

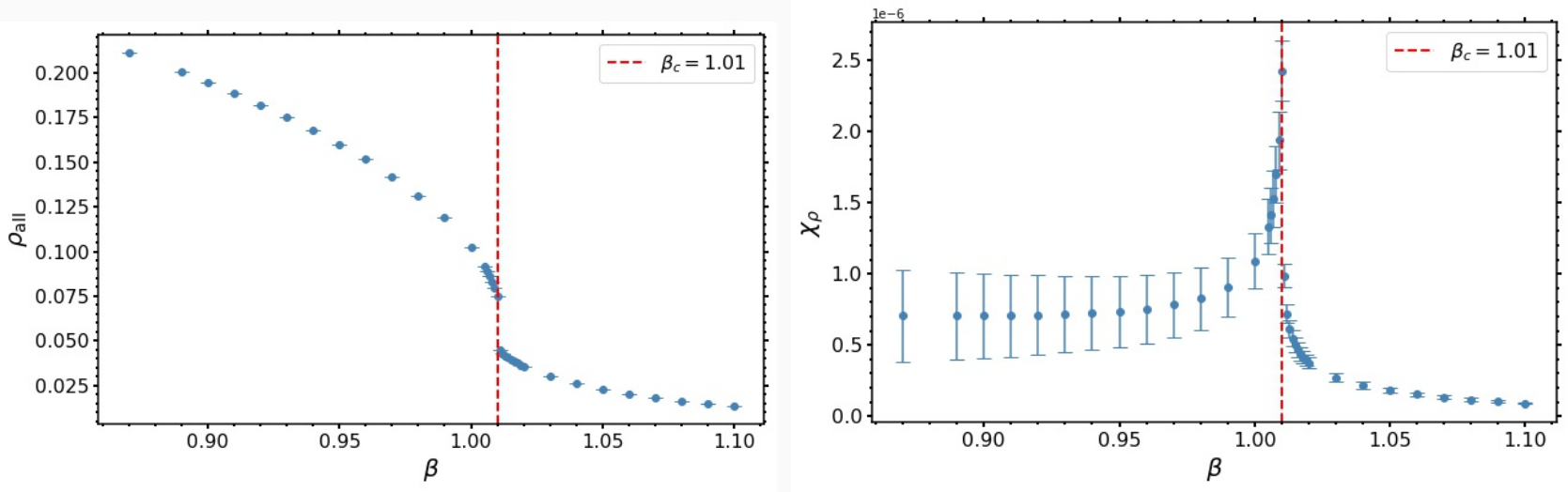

Figure 6: Left: the monopole density ρ vs lattice coupling β; **Right**: its susceptibility. The vertical line marks the position of the phase transition calculated from these observables.

Monopole configurations in the presence of plates

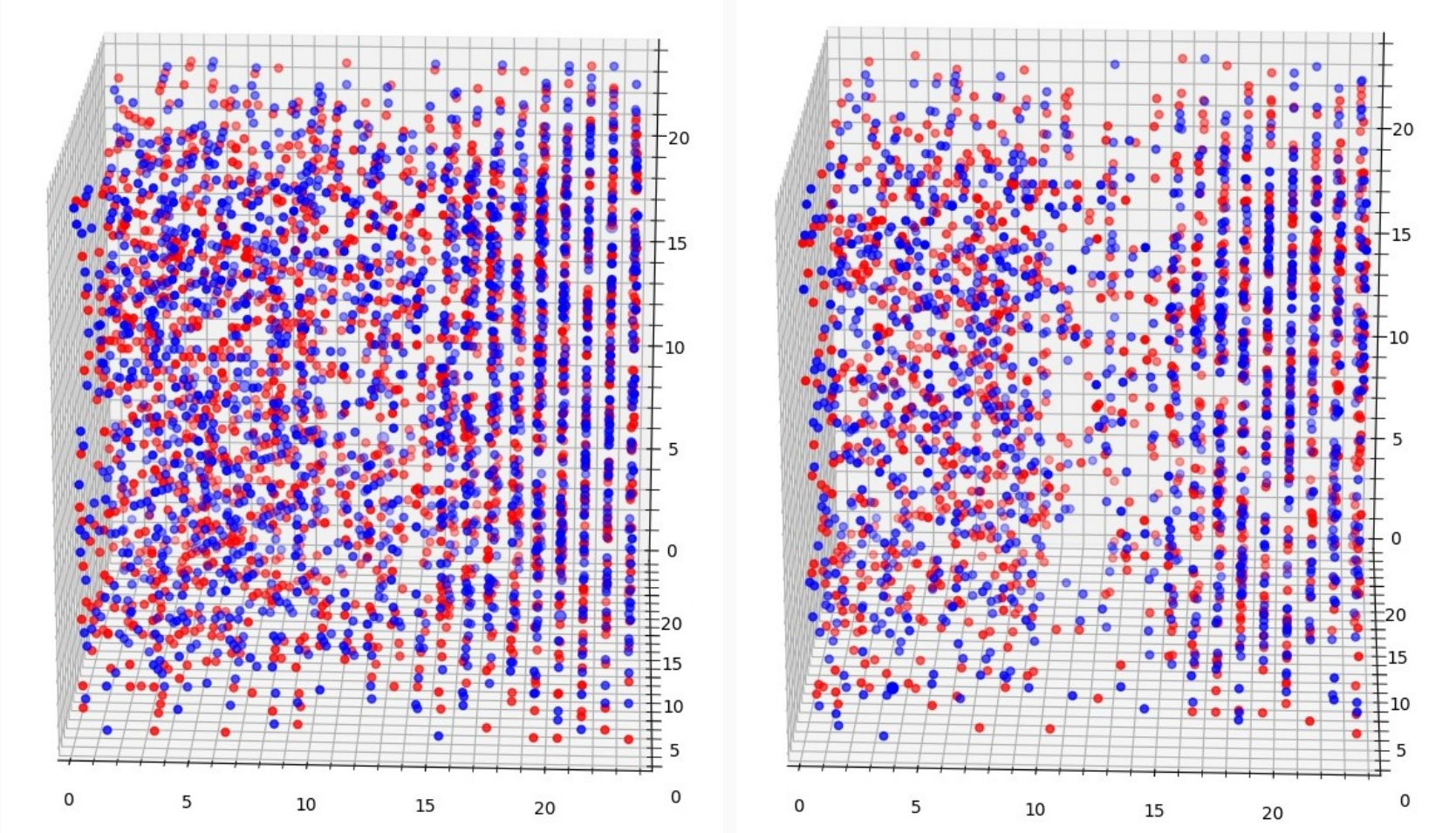

Figure 7: The examples of monopole configurations in the confinement phase(**left**, $\beta = 0.8$) and deconfinement phase (**right**, $\beta = 0.9$) for the plates separated by the distance $R = 3$. Monopoles and antimonopoles are represented by the red and blue dots, respectively. The plates, positioned vertically, are not shown.

The monopole density between plates normalized by monopole density in the absence of plates

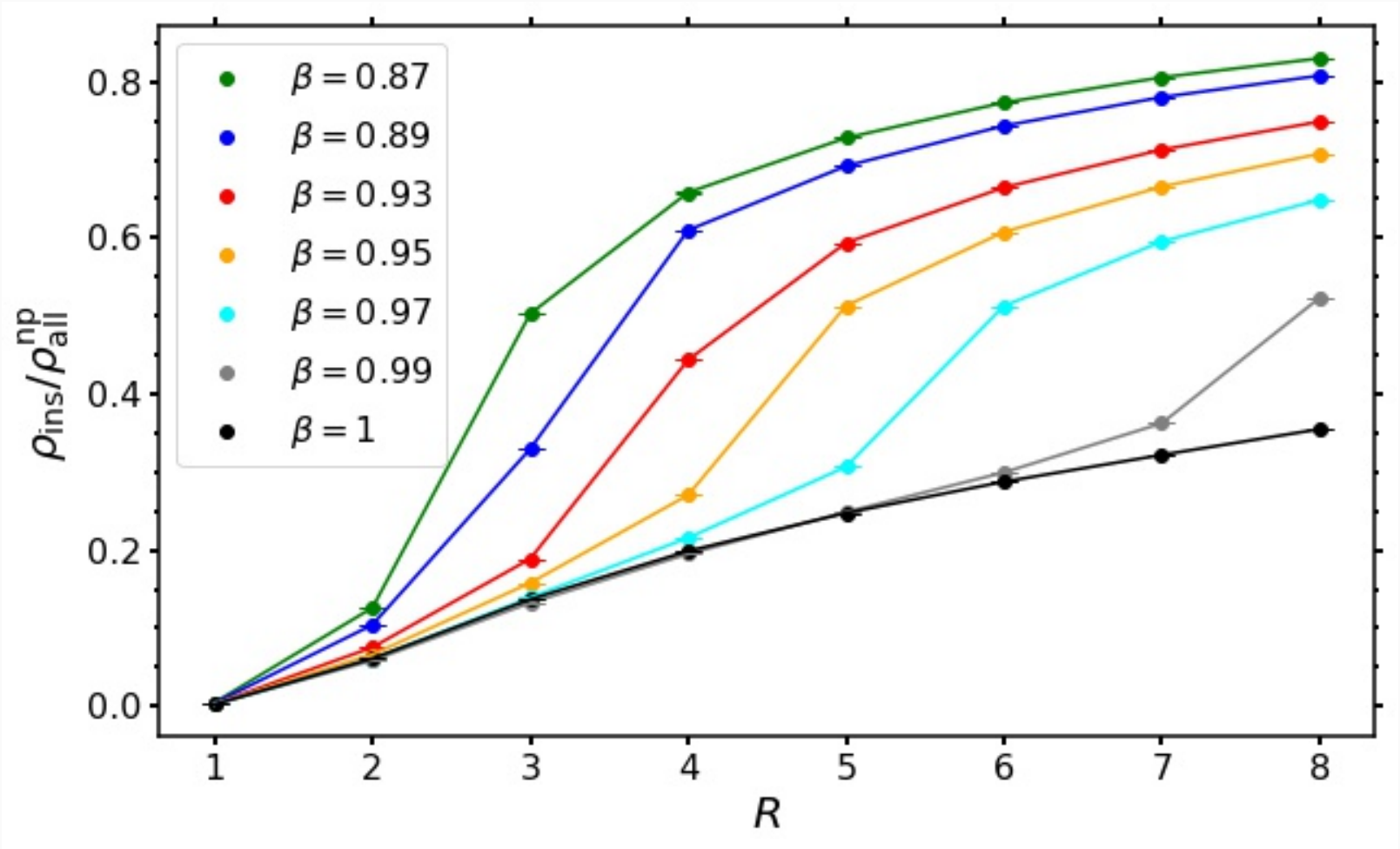

Figure 8: The ratio $\rho_{\rm ins}/\rho^{\rm np}_{\rm ins}$ of the monopole density $\rho_{\rm ins}$ inside the Casimir plates to the monopole density in the absence of the plates, $\rho^{\rm np}_{\rm ins}$ vs interplate separation R for a fixed set of lattice coupling β.

The shift of phase transition point

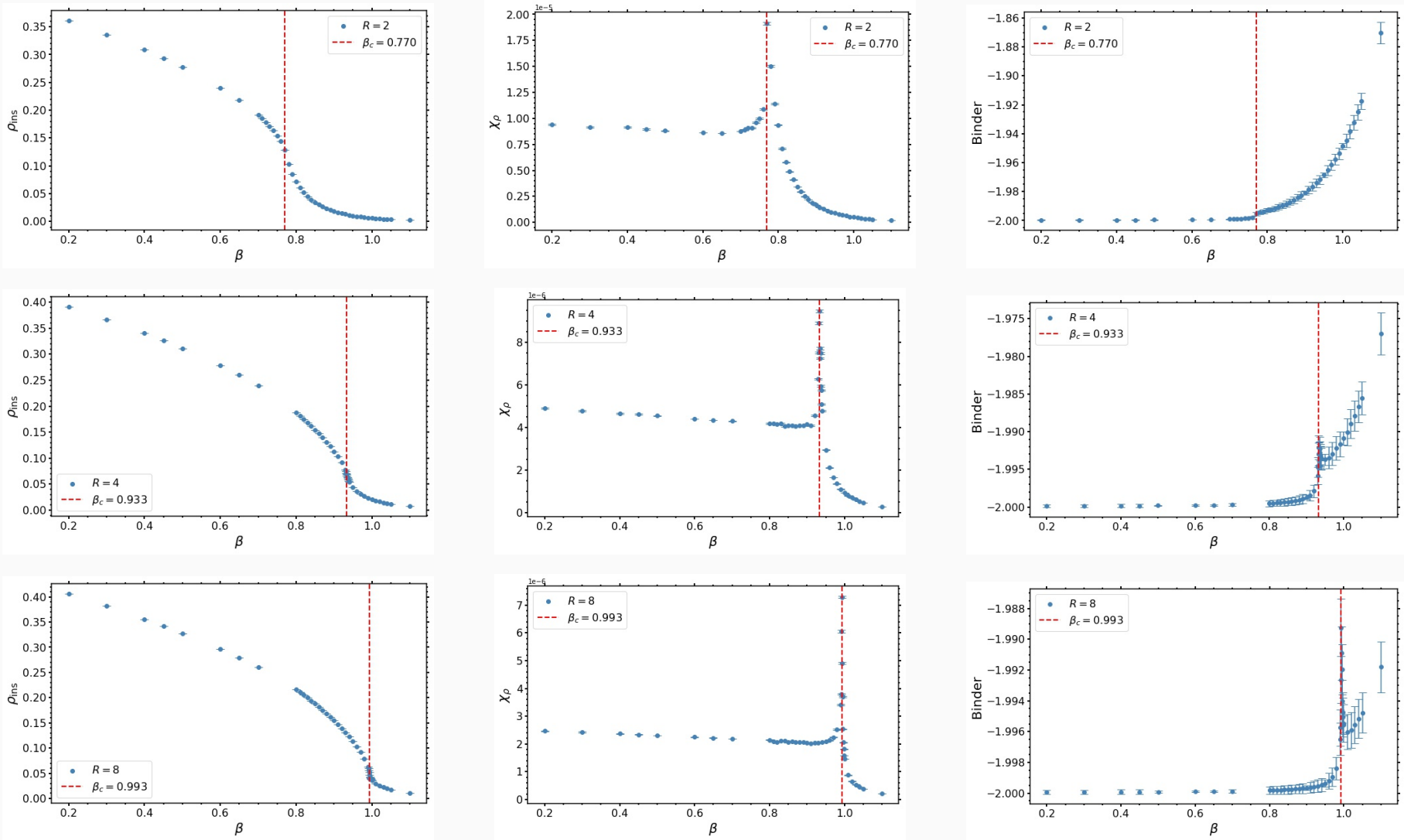

Figure 9: The monopole density (**left**), its susceptibility (**center**) and the Binder cumulant(**right**) for $R = 2, 4, 8$ (from top to bottom).

The phase diagram

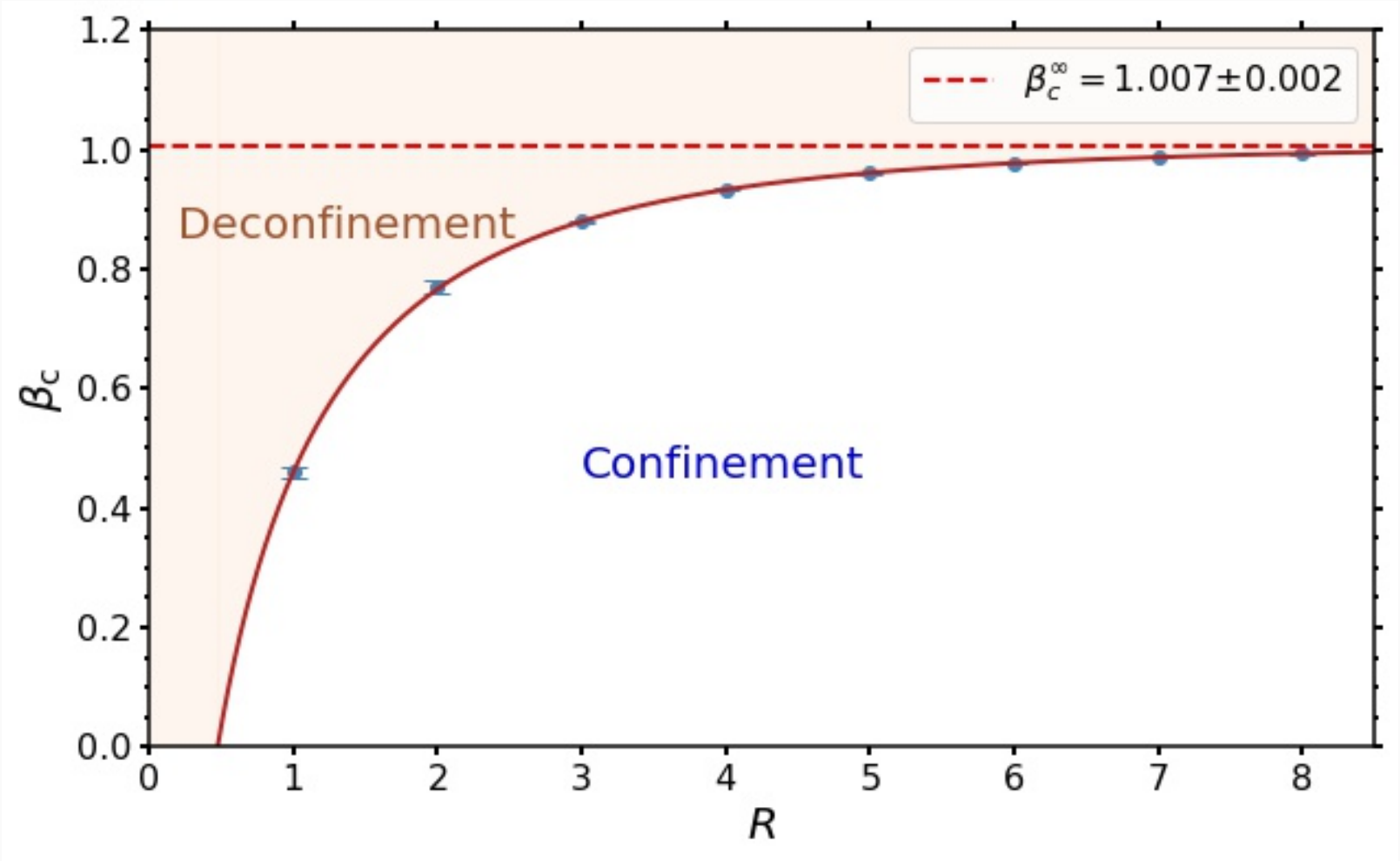

Figure 10: The phase diagram of the vacuum of the compact $U(1)$ gauge theory in between the perfectly metallic plates separated by the distance R. The solid line represents best fit $\beta_c^{\rm fit}(R) = \beta_c^\infty - \alpha \exp[-(R^2/R_0^2)^\nu]$ with $\alpha = 3.7(6)$, $R_0 = 0.28(7)$, $\nu = 0.257(16)$. The limit $R \to \infty$ is shown by the dashed horizontal line.

The Polyakov loop as the deconfinement order parameter

Definitions

$$P_x = \prod_{x_4=0}^{N_T-1} e^{i\theta_{x,x_4;\mu=4}}$$

$$P = \langle P_x \rangle$$

$$|P| = \left| \frac{1}{V_3} \sum_{x \in V_3} P_x \right|$$

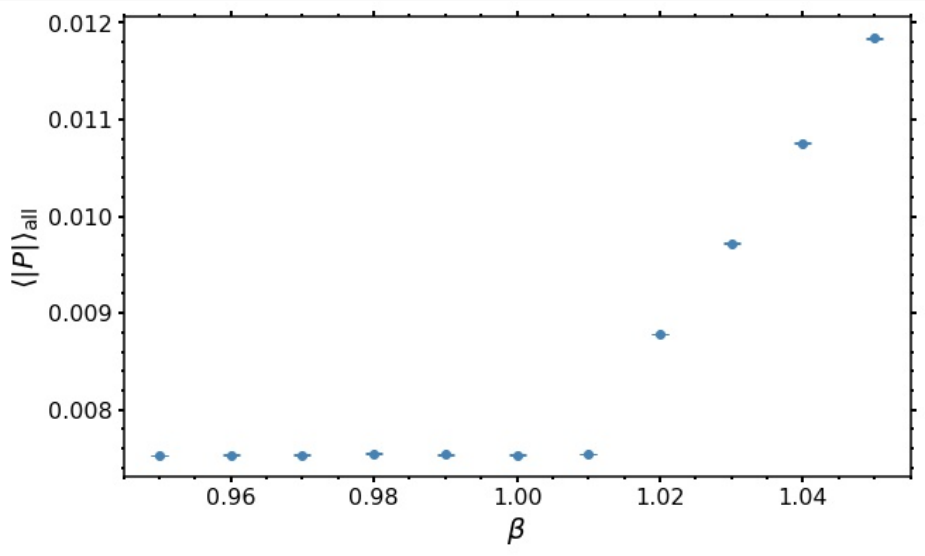

Figure 11: The modulus of Polyakov loop in the absence of plates.

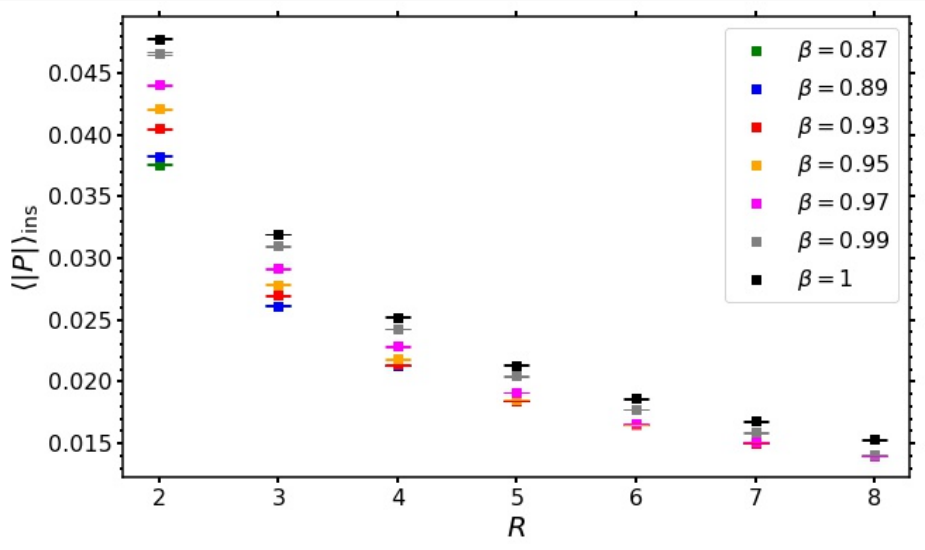

Figure 12: The modulus of the Polyakov loop in the space between the Casimir plates at the separation R at a set of fixed coupling β.

The Polyakov loop inside plates for different R

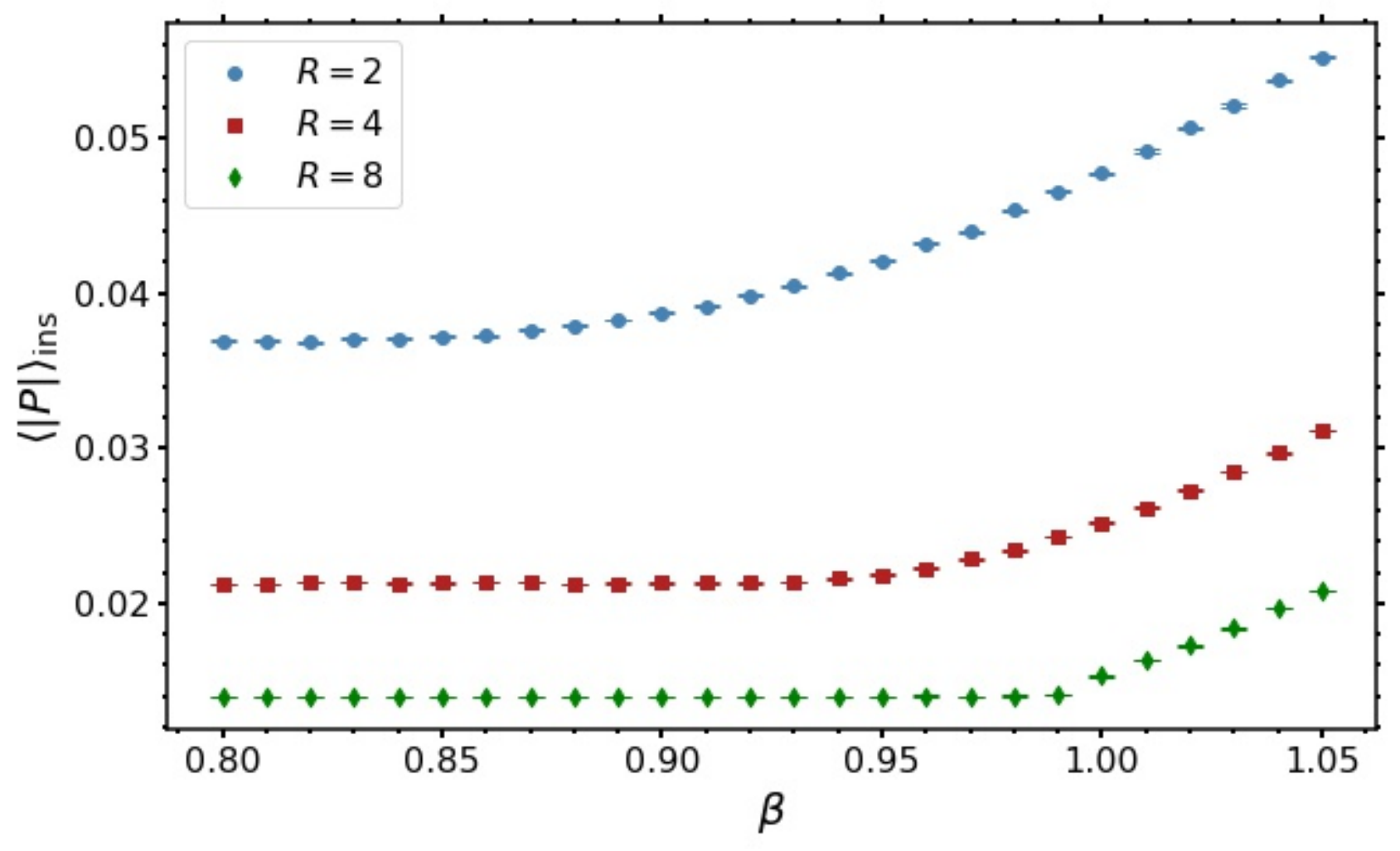

Figure 13: The Polyakov loop inside the plates vs β at fixed R.

The Casimir energy for SU(3) gluodynamics in (3+1)d

Energy-momentum tensor in Minkowski space:

$$T^{\mu\nu} = F^{\mu\alpha}F^{\nu}_{\ \alpha} - \tfrac{1}{4}\eta^{\mu\nu}F^{\alpha\beta}F_{\alpha\beta}$$

Energy density:

$$\mathcal{E} \equiv T^{00} = \tfrac{1}{2}\left(\boldsymbol{B}^2 + \boldsymbol{E}^2\right) \to T^{44}_E = \tfrac{1}{2}\left(\boldsymbol{B}^2_E - \boldsymbol{E}^2_E\right).$$

Lattice Casimir energy density:

$$\mathcal{E}_{\mathrm{Cas}} = \beta L_s\left(\sum_{i=1}^{3}\langle\,\mathcal{P}_{i4}\,\rangle_S - \sum_{i<j=1}^{3}\langle\,\mathcal{P}_{ij}\,\rangle_S\right), \quad \mathcal{P}_{x,ij} = \tfrac{1}{3}\mathrm{Re}\,\mathrm{tr}\,U_{x,ij}$$

Glueton – new boundary state in QCD

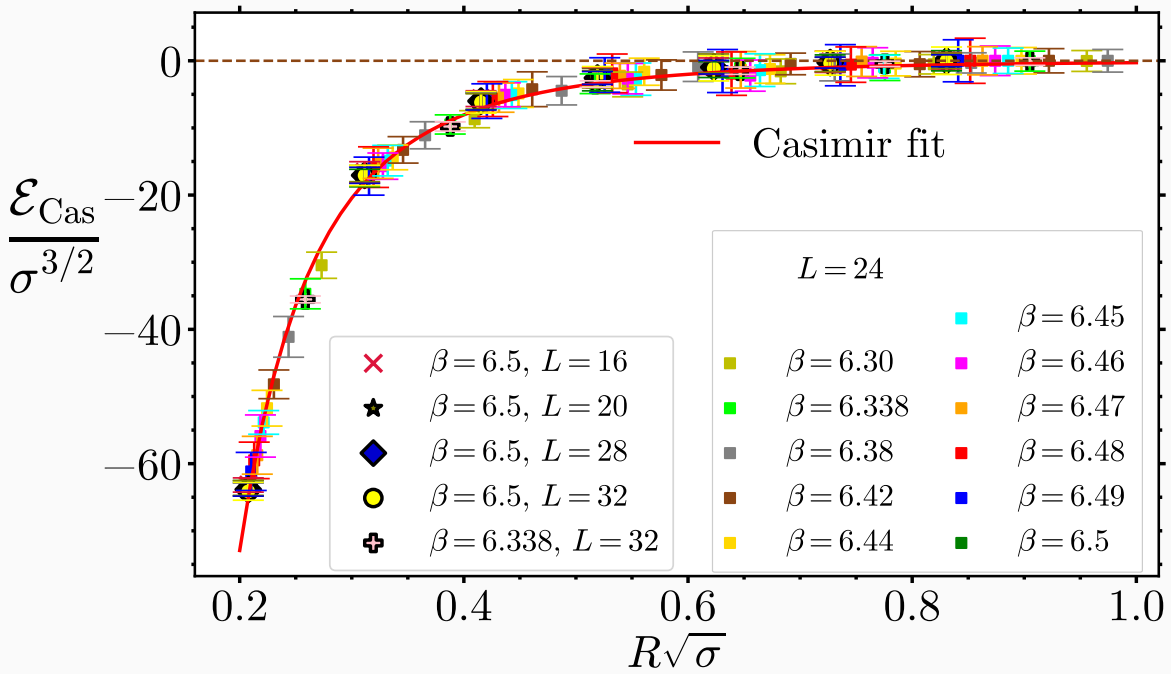

Figure 14: The Casimir energy density $\mathcal{E}_{\rm Cas}$ as function of distance R between chromometallic plates in units of σ.

$$m_{\rm gt} = 1.0(1)\sqrt{\sigma} = 0.49(5)\,\mathrm{GeV}$$

$$M_{0^{++}} = 3.405(21)\sqrt{\sigma} = 1.653(26)\,\mathrm{GeV}$$

(for comparison)

$$\mathcal{E}_{\rm Cas} = -C_0 \frac{2(N_c^2-1)m_{\rm gt}^2}{8\pi^2 R} \sum_{n=1}^{\infty} \frac{K_2(2n m_{\rm gt} R)}{n^2}$$

Quarkiton – a quark bound by a mirror

$F_{Q|}(d)$ – free energy of static quark

$$P_{\boldsymbol{x}} = \frac{1}{3}\mathrm{Re}\,\mathrm{tr}\left(\prod_{x_4=0}^{L_t-1} U_{\boldsymbol{x},x_4}\right)$$

$$\langle P_{\boldsymbol{x}} \rangle_{|}(d) = \exp\left\{-L_T F_{Q|}(d)\right\}$$

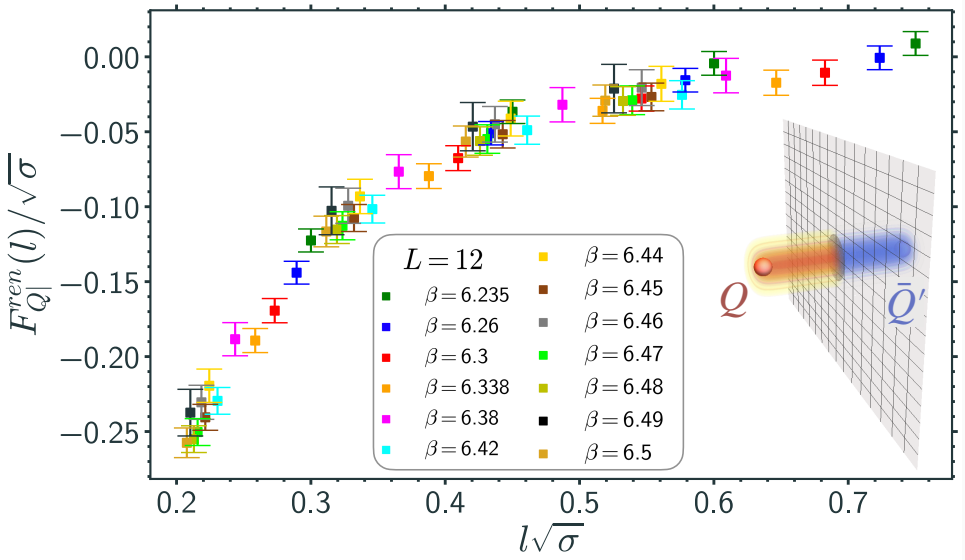

Figure 15: Renormalized free energy of heavy quark $F^{\mathrm{ren}}_{Q|}(l)$ vs distance l from chromometallic mirror in physical units.

Quarkiton interactions

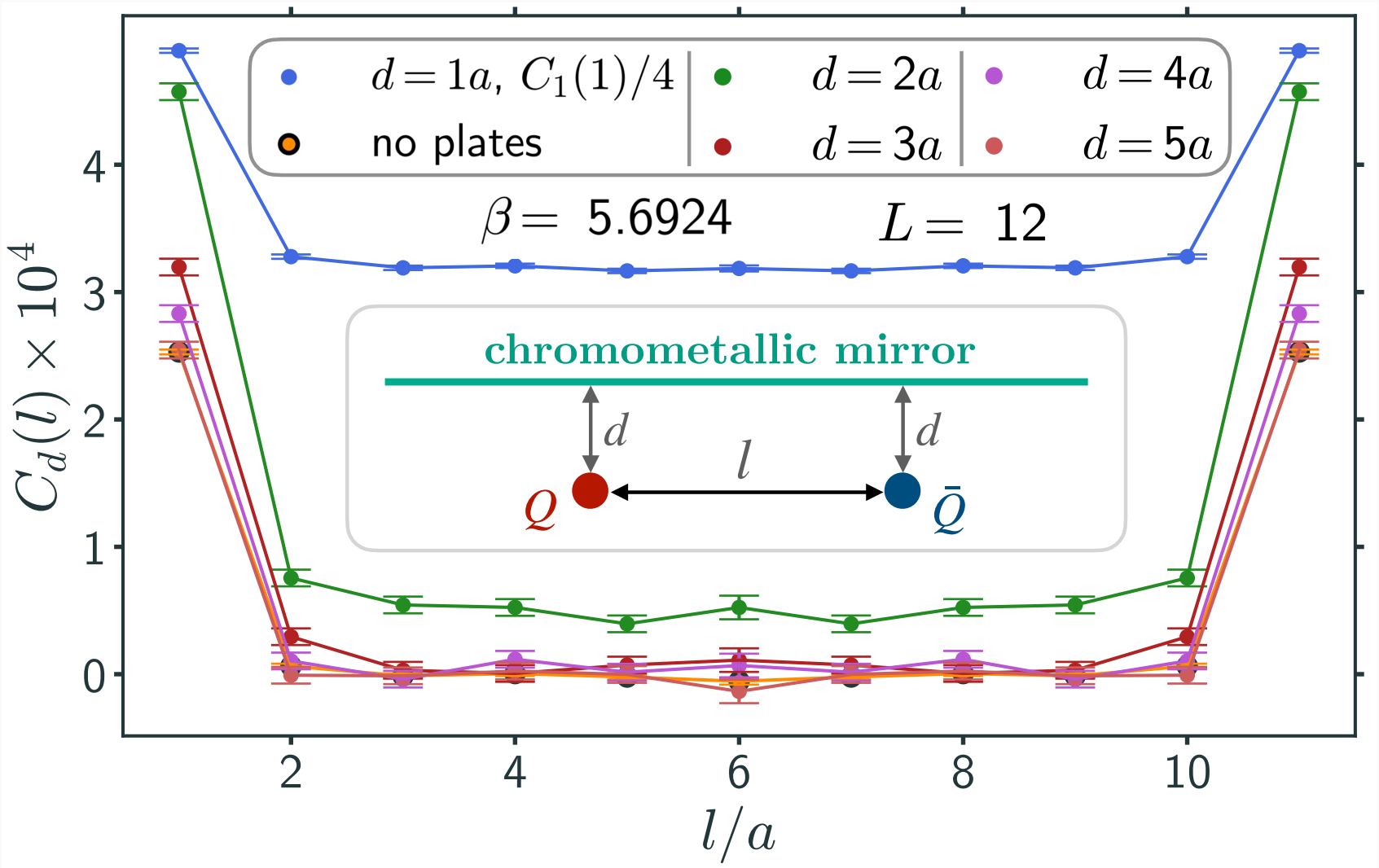

Figure 16: Correlator of Polyakov loops $C_d(l) = \langle P(x)P^*(x+l) \rangle_d$ for quark and antiquark located at distance d from the chromometallic mirror

A heavy quark between non-Abelian mirrors

$$L_T F_Q^{\mathrm{Cas}}(R) = -\ln |P|_{V(R)} \equiv -\ln \left\langle \left| \sum_{\mathbf{x} \in V(R)} P_{\mathbf{x}} \right| \right\rangle$$

$V(R)$ – volume between plates

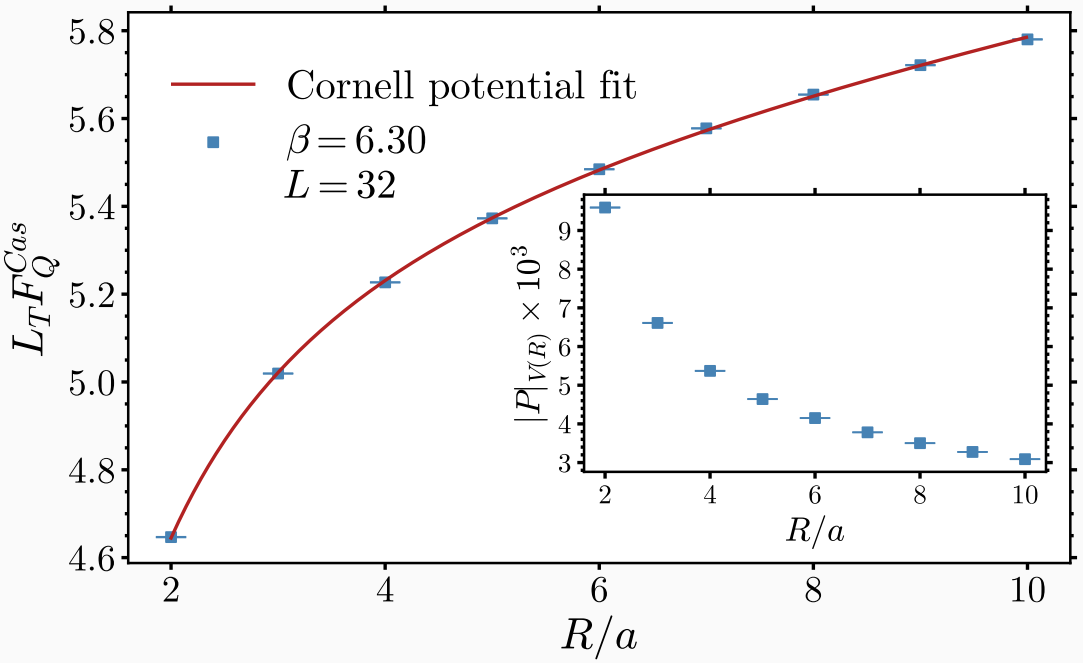

Figure 17: Mean free energy of heavy quark in between the mirrors on the lattice 32^4.

$$L_T F_Q^{\mathrm{Cas}}(R/a) = -\frac{c_1}{R/a} + c_2 \frac{R}{a} + c_0$$

Conclusions

- From first-principle numerical simulations we show that the non-pertubative Casimir effect breaks monopole condensate and induces deconfiment phase transition in between plates for compact QED in (3+1)d
- We observed new colorless boundary state of gluons bounded to their images in mirror with remarkably small mass in YM SU(3) theory in (3+1)d, which we refer as "glueton"
- We qualitatively support the existence of quarkiton – quark bound by the mirror to its negative image
- At short interplate separation a heavy quark in the space between mirrors possesses a finite free energy – deconfiment of a color

Conclusions

- From first-principle numerical simulations we show that the non-pertubative Casimir effect breaks monopole condensate and induces deconfiment phase transition in between plates for compact QED in (3+1)d
- We observed new colorless boundary state of gluons bounded to their images in mirror with remarkably small mass in YM SU(3) theory in (3+1)d, which we refer as "glueton"
- We qualitatively support the existence of quarkiton – quark bound by the mirror to its negative image
- At short interplate separation a heavy quark in the space between mirrors possesses a finite free energy – deconfiment of a color

Thank you for attention!